ACS Sustainable Chemistry & Engineering

Research Article

pubs.acs.org/journal/ascecg

Design of Carbon Black/Polypyrrole Composite Hollow Nanospheres and Performance Evaluation as Electrode Materials for Supercapacitors

Peng Liu,* Xue Wang, and Yunjiao Wang

State Key Laboratory of Applied Organic Chemistry and Key Laboratory of Nonferrous Metal Chemistry and Resources Utilization of Gansu Province, College of Chemistry and Chemical Engineering, Lanzhou University, Lanzhou 730000, China

ABSTRACT: Well-defined carbon black/polypyrrole (CB/PPy) composite hollow nanospheres were prepared via *in situ* chemical oxidative interfacial polymerization of pyrrole in the presence of sulfonic acid-modified carbon black (CB-SO_3H) nanoparticles with inert solvent (toluene) as the soft template, in which sodium dodecyl benzenesulfonate (SDBS) was used as both the surfactant for the emulsion and the dopant for the produced polypyrrole (PPy), as well as the CB-SO_3H nanoparticles. The effects of the preparation conditions, such as the oil/water ratio and feeding ratio of the CB-SO_3H nanoparticles on the morphology, electrical conductivity, and electrochemical properties of the final CB/PPy hollow nanospheres, were investigated. It was found that the CB-SO_3H nanoparticles exhibited an obvious influence on the particle size, electrical conductivity, specific capacitance, and cycling stability of the CB/PPy hollow nanospheres. The highest electrical conductivity and specific capacitance of 0.045 S/cm and 29 F/g were achieved, respectively. After 1000 cycles, the attenuation in the specific capacitance was less than 5%, indicating that the CB/PPy hollow nanospheres possessed excellent cycling performance.

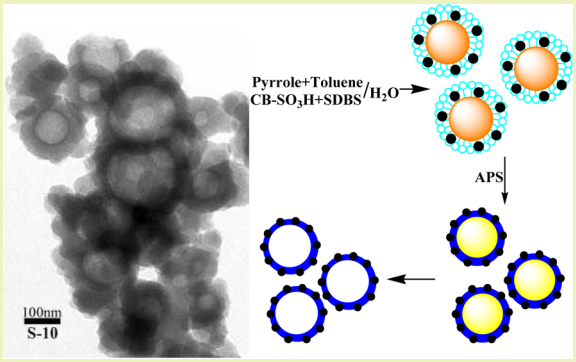

KEYWORDS: *Nanocomposite, Hollow nanospheres, Polypyrrole, Chemical oxidative polymerization, Supercapacitors*

INTRODUCTION

In the last decades, supercapacitors have been widely investigated as an interesting and technologically relevant compromise with respect to power density and energy density.[1] As an important class of electrode materials for supercapacitors, the conductive polymers have attracted more and more interest due to their advantageous properties, such as low cost compared to noble metal oxides, high doping−dedoping rate during charge−discharge process, high charge densities compared to high surface carbon, and easy synthesis through chemical and electrochemical processing.[2,3] However, the lower specific capacitance and lower cycle life of the conductive polymers in comparison with carbon-based electrodes restrict their practical application because the redox sites in the polymer backbone are not sufficiently stable for many repeated redox process.[4] A key point to obtain a high and stable specific capacitance lies on the design of the electroactive materials with better control of their microstructure, such as specific surface area and pore characters, which affects the penetration of the electrolyte into pores, as well as the ion mobility within the conductive polymers.

For polypyrrole (PPy), more and more researchers focused on obtaining a high specific capacitance by preparing PPy nanomaterials (nanospheres,[5] nanotubes,[6] nanofibers,[7] and nanowires[8]) as well as PPy-based nanocomposites[9] with carbon nanoparticles,[10,11] carbon nanotubes,[12,13] graphene,[14,15] nanoclay,[16,17] or nanoscaled oxides[18−20] as supporting materials via chemical oxidative polymerization or electrochemical polymerization. Most recently, the PPy hollow micro/nanospheres have been designed for energy storage. Mangold et al. prepared the electrochemically active PPy hollow microspheres via the chemical oxidative polymerization of pyrrole with iron(0) particles as templates.[21] Yu et al. designed the graphene−hollow PPy nanoarchitecture in which hollow PPy spheres were inserted between graphene layers by mixing graphene oxide and PS@PPy core−shell spheres, followed by reduction of graphene oxide and etching of PS.[22] As an electrode material for supercapacitors, a high specific capacitance of 500 F/g at a charging/discharging current density of 5 A/g was achieved with high cycling stability. It indicated that the tailored nanoarchitecture enhanced the specific surface area of the electrode and promoted the synergetic effect between RGO and PPy, thus leading to a significantly enhanced electrochemical performance.

In our previous work, the carbon nanotube/polypyrrole composite (CNTs/PPy) hollow microspheres were fabricated via chemical oxidative interfacial polymerization of pyrrole in the presence of carbon nanotubes.[23,24] For the carboxylated multiwalled carbon nanotubes (CNT-COOH) with lengths of 120−200 nm by oxidation with a mixture of H_2SO_4/HNO_3

Received: February 16, 2014
Revised: June 12, 2014
Published: June 16, 2014

 © 2014 American Chemical Society

Scheme 1. Formation Mechanism of the Ideal CB/PPy Composite Hollow nanospheres

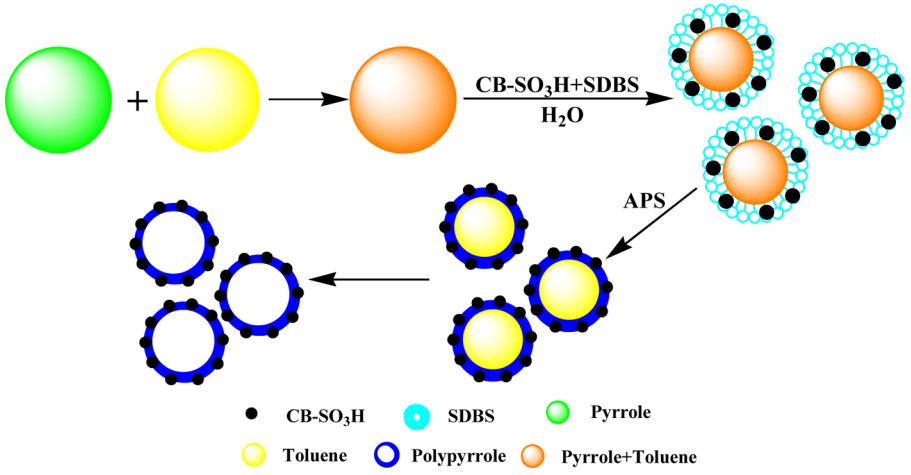

(3:1) for 12 h, the well-defined CNTs/PPy composite hollow microspheres with a near uniform particle size of 1.4 μm were obtained.[23] As in the presence of the benzenesulfonate-modified multiwalled carbon nanotubes (CNT-C_6H_4-SO_3H) with lengths of 0.2−1.4 μm, the hollow PPy nanospheres with particle sizes of about 80 nm were immobilized onto the functional CNTs.[24] It was found that the addition of CNTs had enhanced the electrochemical performance of PPy hollow micro/nanospheres when being used as the electrode materials for supercapacitors.

Here, carbon black nanoparticles (CB, about 40 nm) were used for the preparation of PPy-based composite hollow micro/nanospheres via the chemical oxidative interfacial polymerization of pyrrole (Scheme 1), after being surface modified with sulfonic acid groups, which could make the CB nanoparticles disperse well in water, provide a better interfacial property between the CB nanoparticles and pyrrole, and dope the produced PPy shells.[15,24] The influences of the oil/water ratio and feeding ratio of the CB-SO_3H nanoparticles on the morphology, electrical conductivity, and electrochemical properties of the final CB/PPy hollow nanospheres were investigated.

EXPERIMENTAL METHODS

Materials. Carbon black (CB, about 40 nm) (Yiping Chemical Factory, Shanghai, China) and polyvinylidenefluoride (PVDF) (Funuolin New Chemical Materials Co., Ltd., Zhejiang, China) were used as received.

Pyrrole (Acros Organics) was distilled under reduced pressure after being dehydrated with calcium hydride for 24 h and stored in a refrigerator. Ammonium peroxodisulfate (APS) (Tianjin Chemical Reagent Co., Tianjin, China) as an oxidant and sodium dodecyl benzenesulfonate (SDBS) (Tianjin Guangfu Fine Chemical Research Institute, Tianjin, China) as a surfactant were used as received. Toluene, benzoyl peroxide (BPO), sulfuric acid, and absolute ethanol were purchased from Aladdin Chemical Reagent Co., Ltd. N,N-Dimethylformamide (DMF) (Tianjin Chemical Reagent Co., Tianjin, China) was dehydrated with calcium hydride for 24 h. All other reagents were analytical reagent grade and used without further purification. Double distilled water was used throughout.

Surface Modification of CB Nanoparticles. Typically, CB (3.0 g) and BPO (6.0 g) were dispersed in toluene (300 mL) and heated for 10 h at 80 °C. The CB nanoparticles were filtered and washed with ethanol several times. Finally, the product was dried in vacuum at 50 °C for 24 h to obtain the benzoylated CB (CB-C_6H_5) nanoparticles.

Then a mixture of the CB-C_6H_5 nanoparticles and H_2SO_4 was magnetically stirred for 48 h at 45 °C. The product was neutralized with NaOH aqueous solution and dialysised in deionized water for 48 h. After removing the water by reduced pressure distillation, the sulfonated CB-C_6H_5 (CB-SO_3H) was dried in vacuum at 50 °C for 24 h.

Preparation of CB/PPy Composite Hollow Nanospheres. In a typical procedure, SDBS was dissolved in deionized water, and then the CB-SO_3H nanoparticles were added. After being ultrasonically dispersed, a solution of pyrrole and toluene with different ratios was added. Afterward, the mixture was magnetically stirred for 1 h at 0 °C. As an oxidant, 10 mL aqueous solution containing 1.0 g of APS was added into the above mixture to initiate the chemical oxidative polymerization. The reaction was conducted under magnetic stirring for 10 h. The resulting precipitate was washed with deionized water and ethanol several times. Finally, the product was dried in vacuum at 60 °C for 24 h to obtain the desired CB/PPy composite hollow nanospheres as a dark powder. The polymerizing conditions are summarized in Table 1. For comparison, the PPy hollow nanospheres (S-8) without the CB-SO_3H nanoparticles and the PPy sample (S-12) were also prepared in the same way.

Table 1. Experimental Conditions for CB/PPy Composite Hollow Nanospheres

samples	SDBS (g)	pyrrole (mL)	toluene (mL)	CB-SO_3H (g)	H_2O (mL)	APS (g)
S-1	0.25	0.10	0.50	0.020	60	1.0
S-2	0.25	0.10	0.50	0.020	90	1.0
S-3	0.25	0.10	0.50	0.020	120	1.0
S-4	0.25	0.10	0.20	0.020	90	1.0
S-5	0.25	0.10	0.80	0.020	90	1.0
S-6	0	0.10	0.50	0.020	90	1.0
S-7	0.50	0.10	0.50	0.020	90	1.0
S-8	0.25	0.10	0.50	0	90	1.0
S-9	0.25	0.10	0.50	0.010	90	1.0
S-10	0.25	0.10	0.50	0.030	90	1.0
S-11	0.25	0.10	0.50	0.040	90	1.0
S-12	0.25	0.10	0	0	90	1.0

Characterizations and Testing. The morphologies of the CB/PPy composite hollow nanospheres were characterized with a JEM-1200 EX/S transmission electron microscope (TEM; JEOL, Tokyo, Japan). These samples were dispersed in water in an ultrasonic bath for 30 min and then deposited on a copper grid covered with a perforated carbon film.

dx.doi.org/10.1021/sc5001034 | ACS Sustainable Chem. Eng. 2014, 2, 1795−1801

The Fourier transform infrared (FT-IR) measurements (Impact 400, Nicolet, Waltham, MA) of the samples were carried out in the wavenumber range of 4000−400 cm^{-1} with the KBr pellet method.

Thermogravimetric analysis (TGA) was obtained with a TA Instrument 2050 thermogravimetric analyzer (TA Instrument, New Castle, DE, U.S.A.) at a heating rate of 30 °C/min from room temperature to 800 °C in nitrogen atmosphere.

The electrical conductivities of the CB/PPy composite hollow nanospheres were measured using RTS-2 four-point probe meter (Guangzhou four-point probe meter Electronic Technology Co., Ltd., Guangzhou, China) at ambient temperature. The pellets were obtained by subjecting the powder samples to a pressure of 30 MPa. Each value given is an average of at least three measurements.

The electrochemical measurements were carried out on a CHI660B electrochemical working station (Shanghai Chenhua Instrument Co, Shanghai, China) in 1.0 mol/L H_2SO_4 aqueous solution as electrolyte at ambient temperature. The working electrodes were prepared according to the following steps. An amount of 80 wt % of active materials was mixed with 15 wt % of carbon black in an agate mortar until a homogeneous black powder was obtained. To this mixture, 5 wt % PVDF was added with a few drops of DMF. The resulting paste was uniformly laid on a piece of stainless steel mesh (150 meshes, rinsed with acetone and hydrochloric acid before use) that served as a current collector and then dried at 40 °C for 4 h before use. The stainless steel mesh coated with the CB/PPy composite was pressed for 1 min under 1.0 MPa. The active mass of the composite electrode-based stainless steel mesh was 0.5 mg. A typical three-electrode experimental cell that is equipped with a working electrode, platinum foil counter electrode, and then a saturated calomel reference electrode (SCE) was used to measure the electrochemical properties of the working electrodes.

RESULTS AND DISCUSSION

Surface-Modified CB Nanoparticles. The FT-IR spectra of the CB nanoparticles before and after surface modification

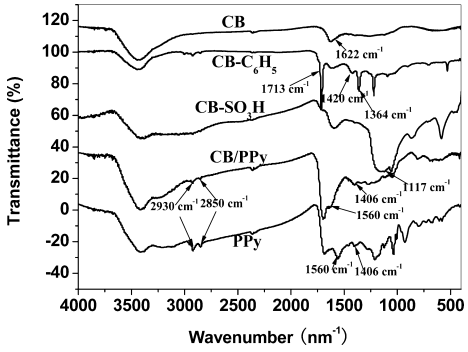

Figure 1. FT-IR spectra of the PPy and CB nanoparticles before and after surface modification (CB-C_6H_5 and CB-SO_3H) and the final CB/PPy composite hollow nanospheres.

(CB-C_6H_5 and CB-SO_3H) were compared in the region of 4000−400 cm^{-1} (Figure 1). In the FT-IR spectrum of the CB-C_6H_5 nanoparticles, the absorbance peak at 1713 cm^{-1} was attributed to the C═O stretching vibration of the benzoyl groups, and those at 1420 and 1364 cm^{-1} were attributed to the stretching vibration of the benzene ring. It declared that the free radical addition reaction took place between the unsaturated groups of the CB nanoparticles and the radicals produced by benzoperoxide.[15,24] As for the CB-SO_3H nanoparticles, the broad characteristic absorbance peak of the aromatic sulfone groups at 1117 cm^{-1} demonstrated that the CB nanoparticles were successfully functionalized with the sulfonic acid groups. After the surface modification, the CB nanoparticles could be

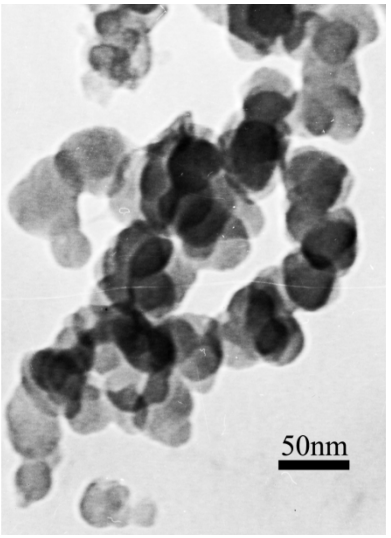

Figure 2. TEM image of the CB-SO_3H nanoparticles.

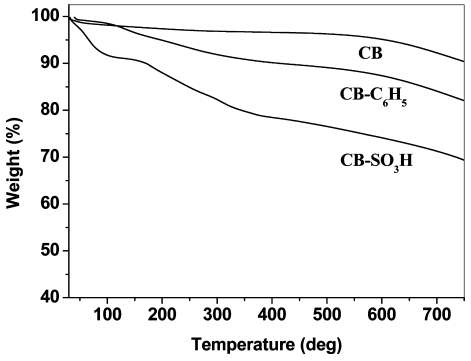

Figure 3. TGA curves of the CB nanoparticles.

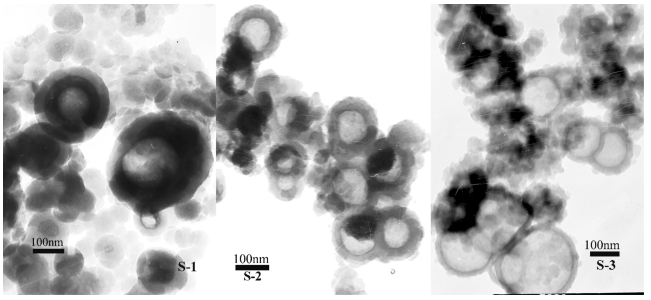

Figure 4. TEM images of the CB/PPy composite hollow nanospheres S-1, S-2, and S-3.

Table 2. Average Diameter and Shell Thickness of CB/PPy Composite Hollow Nanospheres S-1, S-2, and S-3

samples	water (mL)	average outside diameter (nm)	shell thickness (nm)
S-1	60	285	150
S-2	90	163	66
S-3	120	152	43

dispersed well in water, retaining the particle size of about 40 nm (Figure 2).

The weight losses of the CB, CB-C_6H_5, and CB-SO_3H nanoparticles were 1.5%, 7.6%, and 14.5%, respectively, in 200−500 °C from the TGA analysis (Figure 3). So it can be calculated that the mass content of the benzoyl and phenyl

dx.doi.org/10.1021/sc5001034 | ACS Sustainable Chem. Eng. 2014, 2, 1795−1801

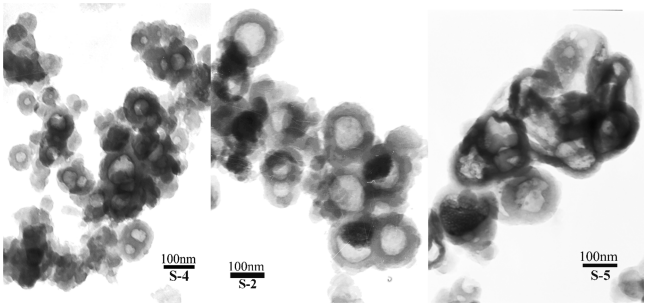

Figure 5. TEM images of the CB/PPy composite hollow nanospheres S-4, S-2, and S-5.

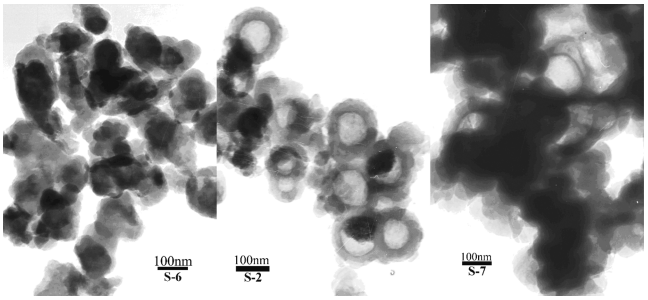

Figure 6. TEM images of the CB/PPy composite hollow nanospheres S-6, S-2, and S-7.

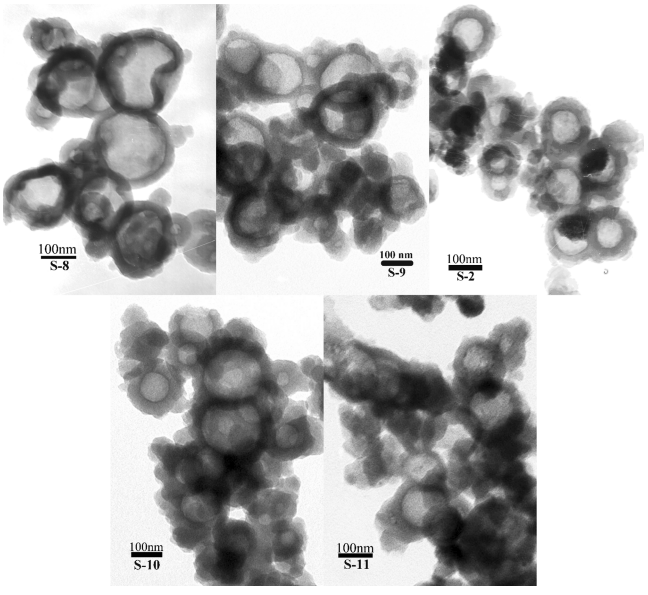

Figure 7. TEM images of the CB/PPy composite hollow nanospheres S-8, S-9, S-2, S-10, and S-11.

groups introduced by benzoylation was about 6.1% in the CB-C_6H_5 nanoparticles, and the mass content of the sulfonic groups by sulfonation was about 6.9% in the CB-SO_3H nanoparticles.

CB/PPy Composite Hollow Nanospheres. Then the well-defined CB/PPy composite hollow nanospheres were prepared via the *in situ* chemical oxidative interfacial polymerization of pyrrole in the presence of the CB-SO_3H nanoparticles with inert solvent (toluene) as the soft template, in which SDBS was used as both the surfactant for the emulsion and the dopant for the final PPy (Scheme 1).[23,25] After the *in situ* chemical oxidative interfacial polymerization, the absorbance at 2850 and 2930 cm^{-1} of the CH stretching modes of PPy appeared in the FT-IR spectrum of the products,[26] revealing the successful polymerization of pyrrole.

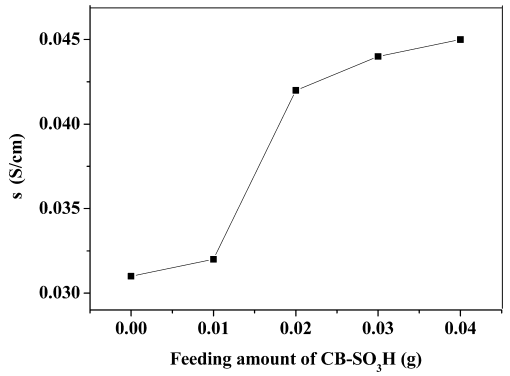

Figure 8. Electrical conductivities of the CB/PPy composite hollow nanosphere samples S-8, S-9, S-2, S-10, and S-11 at room temperature.

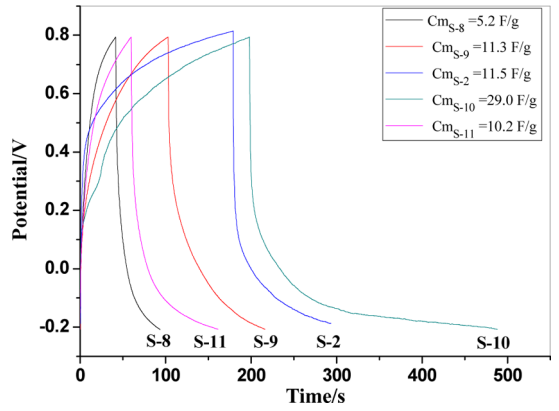

Figure 9. Galvanostatic charge/discharge curves of the CB/PPy composite hollow nanosphere electrodes in 1 mol/L H_2SO_4 at a current density of 0.1 A/g.

The effect of the water amount to the morphology of the CB/PPy composite hollow nanospheres was investigated at first by keeping the dosages of SDBS, pyrrole, toluene, and CB-SO_3H nanoparticles unchanged and only adjusting the dosage of water. It is apparent that the water amount had a strong impact on the size and structure of the composite hollow nanospheres (Figure 4 and Table 2). Few hollow nanospheres were obtained when 60 mL of water was added. It is worth noting that the hollow nanospheres formed two shells at this condition. When the dosage of water reached 90 mL, the size and structure of the hollow nanospheres were uniform. When 120 mL of water was added, the hollow nanospheres became inhomogeneous and the thickness of the shell decreased significantly.

The influence of the amount of toluene was also investigated. On the basis of the TEM images of the CB/PPy composite hollow nanospheres S-4, S-2, and S-5 (Figure 5), it could be concluded that the size of the CB/PPy composite hollow nanospheres was very small when the amount of toluene was 0.2 mL, average diameter was only 80 nm, and average shell thickness was 44 nm. While the amount of toluene was quadrupled, the structure of the CB/PPy composite hollow nanospheres deformed. It declared that toluene was used as the soft template in the polymerization of pyrrole, and the amount of toluene decided the size and stability of the hollow structure.

dx.doi.org/10.1021/sc5001034 | ACS Sustainable Chem. Eng. 2014, 2, 1795−1801

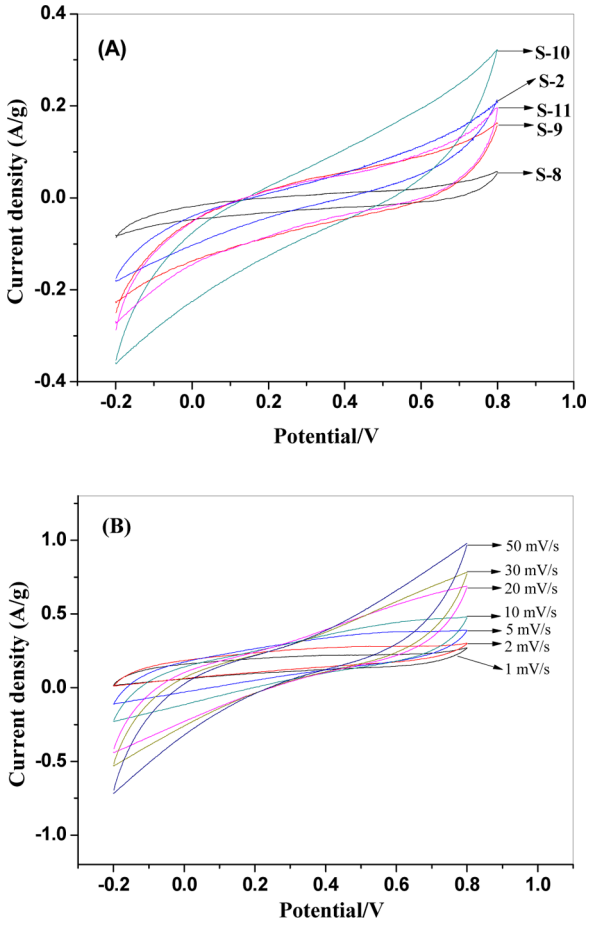

Figure 10. CV curves of the different CB/PPy composite hollow nanosphere electrodes at a scan rate of 10 mV/s (A) and the CB/PPy composite hollow nanospheres S-10 electrode at different scan rates from 1 to 50 mV/s with a potential range between −0.2 and 0.8 V (vs SCE) (B).

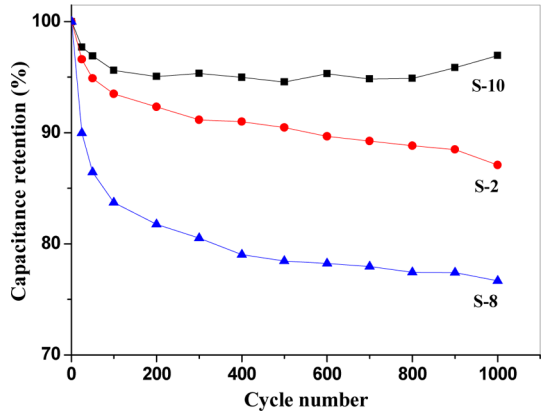

Figure 11. Cycling stability of the CB/PPy composite hollow nanosphere electrodes (samples S-2, S-8, and S-10) between −0.2 and 0.8 V at 100 mV/s.

The influence of the amount of anionic surfactant dosage was investigated by retaining the dosage of pyrrole, toluene, water, and CB-SO_3H nanoparticles. It in shown in Figure 6 that polypyrrole cannot form a hollow structure without adding the anionic surfactant SDBS. However, when the amount of the anionic surfactant increased to 0.5 g, the accumulation of the CB/PPy composite hollow nanospheres also increased. The excess SDBS in water formed the sheet or other shaped micelles.

In conclusion, when the feeding amount of the CB-SO_3H nanoparticles was 0.02 g, the optimum condition for fabricating the CB/PPy composite hollow nanospheres was as follows: 90 mL of water, 0.50 mL of toluene, and 0.25 g of SDBS. On the basis of this, we changed the feeding amount of the CB-SO_3H nanoparticles to investigate its influence on the morphology of the CB/PPy composite hollow nanospheres. The increase in the feeding content of the CB-SO_3H nanoparticles had no remarkable effect on the formation of the CB/PPy composite hollow nanospheres (Figure 7). However, much smoother PPy hollow nanospheres could be obtained without the CB-SO_3H nanoparticles, and the structure of the hollow nanospheres was not stable with collapse in some shells of the hollow nanospheres. It illustrates that the addition of the CB-SO_3H nanoparticles is conducive to stabilizing the structure of the hollow nanospheres, making them more regular. So the CB-SO_3H nanoparticles might play some role as the cosurfactant in interfacial polymerization.[27]

Electrical Conductivity. The electrical conductivities of the CB/PPy composite hollow nanosphere samples S-8, S-9, S-2, S-10, and S-11 at room temperature are presented in Figure 8. The conductivity increased with the increase in feeding content of the CB-SO_3H nanoparticles, and due to that the CB-SO_3H nanoparticles are beneficial for the chain growth of polypyrrole, while the conductivity of the CB/PPy composites depended to the length of the polypyrrole chain. According to the quantum chemistry theory, the longer the conjugated chain is, the lower the electronic activation energy is; thus, the charge carrier can easily be formed under an electric field.[28] The conductivity was 0.025 S/cm for sample S-12 as irregular-shaped aggregates, which was not a hollow structure and was without the CB-SO_3H nanoparticles. It also confirmed that the hollow structure can enhance the conductivity effectively.[29]

Electrochemical Performance. To investigate the electrochemical behaviors of the CB/PPy composite hollow nanospheres, the samples were fabricated into the working electrodes. The electrochemical behaviors of the CB/PPy composite hollow nanosphere electrodes were investigated using galvanostatic charging/discharging (GCD) and cyclic voltammetry (CV) techniques. The specific capacitance (Cm) can be calculated according to $Cm=(\int IdV)/(mV\upsilon)$, where Cm is the specific capacitance, I is the response current density, V is the potential window, υ is the potential scan rate, and m is the mass of the active material in the working electrode.

Figure 9 shows the galvanostatic charging/discharging (GCD) curves of the CB/PPy composite hollow nanosphere electrodes in 1 mol/L H_2SO_4 at a current density of 0.1 A/g. It is shown that the curves of the CB/PPy composite hollow nanosphere electrodes are not ideal symmetric profiles, exhibiting the following two voltage stages. The former voltage stage with a short discharging duration is ascribed to the electric double-layer (EDL) capacitance of the electrodes, whereas the latter voltage stage with a longer discharging duration is attributed to the combination of the EDL and Faradaic capacitances from the redox transition of PPy.[30,31] The specific capacitance increased with increasing the feeding amount of the CB-SO_3H nanoparticles up to 0.030 g for the CB/PPy composite hollow nanosphere sample 10 with the highest specific capacitance value of 29 F/g, which decreased afterward.

The galvanostatic charge/discharge curves of the CB/PPy composite hollow nanosphere electrodes showed large IR drops

dx.doi.org/10.1021/sc5001034 | ACS Sustainable Chem. Eng. 2014, 2, 1795−1801

in the beginning of each discharge curve. The IR drop of the pure PPy hollow nanospheres electrodes (S-8) was 0.32 V. Introducing the CB-SO_3H nanoparticles decreased the IR drops of the CB/PPy composite hollow nanosphere electrodes, mainly due to the increased electrical conductivity and reduced internal resistance.[31] Moreover, the electrical conductivity of the CB/PPy composite hollow nanospheres increased as the IR drop decreased (Figure 8). It is clear that S-10 with the lowest IR drop of 0.18 V possessed the highest specific capacitance.

Figure 10 shows a series of the CV curves of the different CB/PPy composite hollow nanosphere electrodes at scan rate of 10 mV/s (Figure 10 A) and the CB/PPy composite hollow nanospheres S-10 electrode at different scan rates from 1 to 50 mV/s with a potential range between −0.2 and 0.8 V (vs SCE) (Figure 10 B). It can be observed that the CV curves of all electrodes showed the rectangle-like shape without obvious redox peaks, revealing that the CB/PPy composite hollow nanosphere electrodes possessed pure electrical double-layer (EDL) capacitance,[32] even at low scan rate of 1 mV/s.

The cycling stability of the CB/PPy composite hollow nanosphere electrodes (samples S-2, S-8, and S-10) were compared using CV curves between −0.2 and 0.8 V at 100 mV/s (Figure 11). The CB/PPy composite hollow nanosphere electrodes (samples S-2 and S-10) showed improved cycling stability compared to that of the PPy hollow nanosphere electrode (sample S-8). In particular, the specific capacitance of the CB/PPy composite hollow nanosphere sample S-10 still remained at a high level of more than 95%. It indicated that the addition of a certain amount of the CB-SO_3H nanoparticles could enhance the electric conductivity, specific capacitance, and cycling stability of the CB/PPy composite hollow nanospheres due to their stabilizing and doping effects.

CONCLUSIONS

A facile approach was developed for the fabrication of well-defined CB/PPy composite hollow nanospheres via chemical oxidative interfacial polymerization of pyrrole in the presence of CB-SO_3H nanoparticles. It was found that the presence of CB-SO_3H nanoparticles greatly improved their morphological, electrical conductive, and capacitance properties. The cycling stability as electrode materials for supercapacitors had been evidently improved by introducing the CB-SO_3H nanoparticles. It makes the CB/PPy composite hollow nanospheres potential electrode materials for supercapacitors.

AUTHOR INFORMATION

Corresponding Author

* E-mail: pliu@lzu.edu.cn. Tel./Fax: 86-931-8912582.

Notes

The authors declare no competing financial interest.

ACKNOWLEDGMENTS

This work was supported by the Natural Science Foundation of Gansu Province (Grant No. 1107RJZA213) and the Fundamental Research Funds for the Central Universities (Nos. lzujbky-2011-21 and lzujbky-2013-237).

REFERENCES

(1) Arico, A. S.; Bruce, P.; Scrosati, B.; Tarascom, J. M.; van Schalwijk, W. Nanostructured materials for advanced energy conversion and storage devices. *Nat. Mater.* **2005**, *4*, 366−377.

(2) Simon, P.; Gogotsi, Y. Materials for electrochemical capacitors. *Nat. Mater.* **2008**, *7*, 845−854.

(3) Ramya, R.; Sivasubramanian, R.; Sangaranarayanan, M. V. Conducting polymers-based electrochemical supercapacitors—Progress and prospects. *Electrochim. Acta* **2011**, *196*, 1−12.

(4) Ghosh, S.; Bowmaker, G. A.; Cooney, R. P.; Seakins, J. M. Infrared and Raman spectroscopic studies of the electrochemical oxidative degradation of polypyrrole. *Synth. Met.* **1998**, *95*, 63−67.

(5) Ghamouss, F.; Brugere, A.; Anbalagan, A. C.; Schmaltz, B.; Luais, E.; Tran-Van, F. Novel glycerol assisted synthesis of polypyrrole nanospheres and its electrochemical properties. *Synth. Met.* **2013**, *168*, 9−15.

(6) Wang, J. G.; Wei, B. Q.; Kang, F. Y. Facile synthesis of hierarchical conducting polypyrrole nanostructures via a reactive template of MnO_2 and their application in supercapacitors. *RSC Adv.* **2014**, *4*, 199−202.

(7) Ghenaatian, H. R.; Mousavi, M. F.; Rahmanifar, M. S. High performance hybrid supercapacitor based on two nanostructured conducting polymers: Self-doped polyaniline and polypyrrole nanofibers. *Electrochim. Acta* **2012**, *78*, 212−222.

(8) Zhang, H. R.; Wang, J. X.; Shan, Q. J.; Wang, Z.; Wang, S. C. Tunable electrode morphology used for high performance supercapacitor: Polypyrrole nanomaterials as model materials. *Electrochim. Acta* **2013**, *90*, 535−541.

(9) Liu, P. Polypyrrole/Inorganic Nanocomposites for Supercapacitors. In *Conducting Polymer Based Blends and Nanocomposites: Synthesis, Properties, and Applications*; Saini, P., Ed.; Scrivener Publishing LLC: Beverly, MA, 2014.

(10) Yang, C.; Liu, P.; Wang, T. M. Well-defined core−shell carbon black/polypyrrole nanocomposites for electrochemical energy storage. *ACS Appl. Mater. Interface* **2011**, *3*, 1109−1114.

(11) An, H. F.; Wang, Y.; Wang, X. Y.; Zheng, L. P.; Wang, X. Y.; Yi, L. H.; Bai, L.; Zhang, X. Y. Polypyrrole/carbon aerogel composite materials for supercapacitor. *J. Power Source* **2010**, *195*, 6964−6969.

(12) Shi, K. Y.; Zhitomirsky, I. Fabrication of polypyrrole-coated carbon nanotubes using oxidant-surfactant nanocrystals for supercapacitor electrodes with high mass loading and enhanced performance. *ACS Appl. Mater. Interface* **2013**, *5*, 13161−13170.

(13) Paul, S.; Choi, K. S.; Lee, D. J.; Sudhagar, P.; Kang, Y. S. Factors affecting the performance of supercapacitors assembled with polypyrrole/multi-walled carbon nanotube composite electrodes. *Electrochim. Acta* **2012**, *78*, 649−655.

(14) Lai, L. F.; Wang, L.; Yang, H. P.; Sahoo, N. G.; Tam, Q. X.; Liu, J. L.; Poh, C. K.; Lim, S. H.; Shen, Z. X.; Lin, J. Y. Tuning graphene surface chemistry to prepare graphene/polypyrrole supercapacitors with improved performance. *Nano Energy* **2012**, *1*, 723−731.

(15) Wang, X.; Yang, C.; Li, H. D.; Liu, P. Synthesis and electrochemical performance of well-defined flake-shaped sulfonated graphene/polypyrrole composites via facile in situ doping polymerization. *Electrochim. Acta* **2013**, *111*, 729−737.

(16) Chang, Y.; Liu, Z. H.; Fu, Z. B.; Wang, C. Y.; Dai, Y. T.; Peng, R. F.; Hu, X. P. Preparation and characterization of one-dimensional core-shell sepiolite/polypyrrole nanocomposites and effect of organic modification on the electrochemical properties. *Ind. Eng. Chem. Res.* **2014**, *53*, 38−47.

(17) Wang, Y. J.; Liu, P.; Yang, C.; Mu, B.; Wang, A. Q. Improving capacitance performance of attapulgite/polypyrrole composites by introducing rhodamine B. *Electrochim. Acta* **2013**, *89*, 422−428.

(18) Bahloul, A.; Nessark, B.; Briot, E.; Groult, H.; Mauger, A.; Zaghib, K.; Julien, C. M. Polypyrrole-covered MnO_2 as electrode material for supercapacitor. *J. Power Source* **2013**, *240*, 267−272.

(19) Amarnath, C. A.; Ghamouss, F.; Schmaltz, B.; Autret-Lambert, C.; Roger, S.; Gervais, F.; Tran-Van, F. Polypyrrole/lanthanum strontium Manganite oxide nanocomposites: Elaboration and characterization. *Synth. Met.* **2013**, *167*, 18−24.

(20) Lee, H.; Cho, M. S.; Kim, I. H.; Nam, J. D.; Lee, Y. RuO_x/polypyrrole nanocomposite electrode for electrochemical capacitors. *Synth. Met.* **2010**, *160*, 1055−1059.

(21) Mangold, K. M.; Schuster, J.; Weidlich, C. Synthesis and properties of magnetite/polypyrrole core−shell nanocomposites and polypyrrole hollow spheres. *Electrochim. Acta* **2011**, *56*, 3616−3619.

(22) Zgang, J.; Yu, Y.; Liu, L.; Wu, Y. Graphene−hollow PPy sphere 3D-nanoarchitecture with enhanced electrochemical performance. *Nanoscale* **2013**, *5*, 3052−3057.
(23) Liu, P.; Wang, X.; Li, H. D. Preparation of carboxylated carbon nanotubes/polypyrrole composite hollow microspheres via chemical oxidative interfacial polymerization and their electrochemical performance. *Synth. Met.* **2013**, *181*, 72−78.
(24) Liu, P.; Wang, X.; Li, H. D. Facile preparation of string-like composite of hollow PPy nanospheres decorated on the carbon nanotubes. *Synth. Met.* **2014**, *189*, 173−176.
(25) Zhang, L.; Liu, P.; Ju, L. L.; Wang, L.; Zhao, S. N. Polypyrrole nanocapsules via interfacial polymerization. *Macromol. Res.* **2013**, *18*, 648−652.
(26) Kato, H.; Nishikawa, O.; Matsui, T.; Honma, S.; Kokado, H. Fourier transform infrared spectroscopy study of conducting polymer polypyrrole: higher order structure of electrochemically-synthesized film. *J. Phys. Chem.* **1991**, *95*, 6014−6016.
(27) Zhang, L.; Liu, P.; Wang, T. M. Preparation of superparamagnetic polyaniline hybrid hollow microspheres in oil/water emulsion with magnetic nanoparticles as cosurfactant. *Chem. Eng. J.* **2011**, *171*, 711−716.
(28) Zhu, C. E.; Ren, L.; Wang, L. X.; An, H. Y. Preparation of polypyrrole/carbon black conductive composites by adsorption polymerization. *Acta Mater. Compos. Sin.* **2005**, *22*, 45−48.
(29) Cai, Z. H.; Martin, C. R. Electronically conductive polymer fibers with mesoscopic diameters show enhanced electronic conductivities. *J. Am. Chem. Soc.* **1989**, *111*, 4138−4139.
(30) Yao, W.; Zhou, H.; Lu, Y. Synthesis and property of novel MnO_2@polypyrrole coaxial nanotubes as electrode material for supercapacitors. *J. Power Sources* **2013**, *241*, 359−366.
(31) Liu, A. R.; Li, C.; Bai, H.; Shi, G. Q. Electrochemical deposition of polypyrrole/sulfonated graphene composite films. *J. Phys. Chem. C* **2010**, *114*, 22783−22789.
(32) Fang, Y.; Luo, B.; Jia, Y. Y.; Li, X. L.; Wang, B.; Song, Q.; Kang, F. Y.; Zhi, L. J. Renewing functionalized graphene as electrodes for high-performance supercapacitors. *Adv. Mater.* **2012**, *24*, 6348−6355.